Photoassociation of Sodium in a Bose-Einstein Condensate

C. McKenzie, J. Hecker Denschlag,* H. Häffner,* A. Browaeys, Luís E. E. de Araujo,† F. K. Fatemi,‡ K. M. Jones,§ J. E. Simsarian,‖ D. Cho,¶ A. Simoni,** E. Tiesinga, P. S. Julienne, K. Helmerson, P. D. Lett, S. L. Rolston, and W. D. Phillips

National Institute of Standards and Technology, Gaithersburg, Maryland 20899

(Received 27 November 2001; published 7 March 2002)

We form ultracold Na_2 molecules by single-photon photoassociation of a Bose-Einstein condensate, measuring the photoassociation rate, linewidth, and light shift of the $J = 1$, $v = 135$ vibrational level of the $A^1\Sigma_u^+$ molecular state. The photoassociation rate constant increases linearly with intensity, even where it is predicted that many-body effects might limit the rate. Our observations are in good agreement with a two-body theory having no free parameters.

DOI: 10.1103/PhysRevLett.88.120403 PACS numbers: 03.75.Fi, 33.20.Kf, 33.70.Jg, 34.20.Cf

Bose-Einstein condensates (BECs) of atomic gases [1,2] are versatile systems for the study of quantum behavior. Of particular interest are the suggestions for the coherent coupling of a BEC of atoms with a BEC of molecules [3–6] and the possibility of creating entangled atoms via coupling with molecular levels [7]. Photoassociation processes using stimulated Raman transitions have formed ground state molecules from ground state atoms in a BEC [8,9], but at very low rates. Here we explore the fundamental upper limits of molecule formation by making them at high rates using the elementary process of single-photon photoassociation.

In single-photon photoassociation, two atoms collide in the presence of a light field and form an excited state molecule. Photoassociative spectroscopy is used extensively to study collisions between laser-cooled atoms [10]. Photoassociation in a BEC presents quite a different regime: The collision energies are orders of magnitude lower than in a laser-cooled sample (the de Broglie wavelength is as big as the sample) and the densities are higher. This puts us in a regime where many-body effects may be important.

We concentrate on a particular photoassociation transition and measure the photoassociation spectra for various intensities and durations of the light pulse. From these, we determine the photoassociation rate, line shape, and the shift of the resonance. Finally, we examine various limits on the photoassociation rate.

Figure 1 shows the photoassociation process. The molecular level chosen for study is the $J = 1$, $v = 135$, rotational-vibrational level of the $A^1\Sigma_u^+$ Na_2 molecular state, excited from free atoms by a laser frequency of 16 913.37(2) cm^{-1} [11]. We chose this level because its detuning from the D_1 resonance is far enough (43 cm^{-1}) for atomic absorption to be negligible and because our experiments in a magneto-optical trap indicated a high photoassociation rate. The lifetime of our excited molecules is about 8.6 ns. The immediate decay of excited molecules into hot atoms or ground state molecules constitutes loss from the condensate. This loss is how we detect photoassociation.

We prepare an almost pure condensate of $N \approx 4 \times 10^6$ sodium atoms in the $|F = 1, m_F = -1\rangle$ ground state with a peak density of $n_0 \approx 4 \times 10^{14}$ cm^{-3}. The condensate is held in an anisotropic time-averaged orbiting potential (TOP) [12] magnetic trap with oscillation frequencies of $\omega_x/\sqrt{2} = \omega_y = \sqrt{2}\,\omega_z = 2\pi \times 198$ Hz and corresponding Thomas-Fermi radii of $\sqrt{2}\,r_x = r_y = r_z/\sqrt{2} = 15$ μm.

To induce photoassociation, we illuminate the BEC with a Gaussian laser beam focused to 120 μm FWHM at the condensate. The peak intensity is varied from 50 to 1200 W cm^{-2}. The polarization is linear and parallel with the rotation (z) axis of the TOP trap bias field. The light is applied as a square pulse for between 10 and 400 μs with rise and fall times less than 0.5 μs.

The condensate number is measured using phase contrast imaging [13], taking two images before and two images after the photoassociation pulse to determine loss. The imaging occurs at 40 ms intervals using a 100 μs

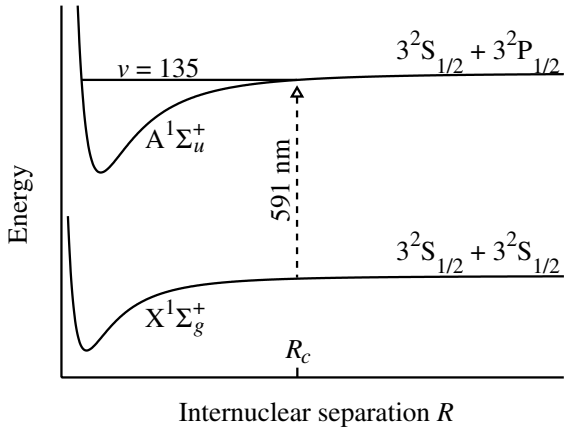

FIG. 1. The two-atom potentials for the ground state and the excited state used for photoassociation. The atoms are initially unbound and on the ground state asymptote and are excited into the $J = 1$, $v = 135$ level. From there they decay and are lost from the condensate. $R_C = 2.0$ nm is the Condon radius, the internuclear separation where the energy of a resonant photon matches the difference between the potentials.

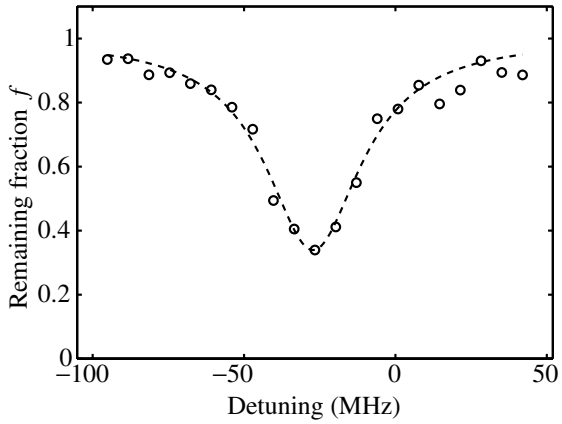

FIG. 2. A typical photoassociation loss spectrum. A 140 W cm^{-2} pulse was applied for 100 μs. The dotted line is a fit to Eq. (2). The uncertainty in the frequency for each point is 5 MHz.

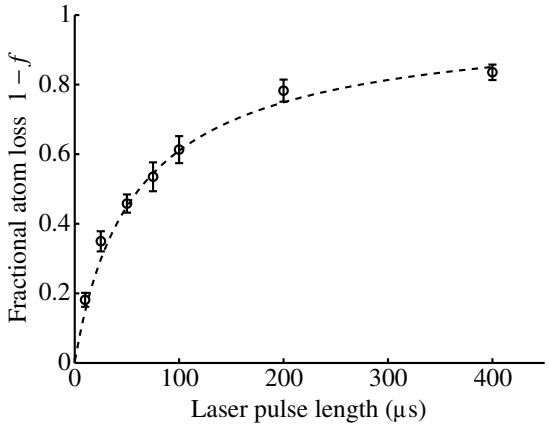

FIG. 3. The dependence of the maximum condensate loss on the photoassociation pulse length for $I = 140$ W cm^{-2}; the curve is a fit of Eq. (2).

probe pulse from a laser tuned 1.78 GHz to the red of the $3S_{1/2}$, $F = 1 \rightarrow 3P_{3/2}$, $F = 2$ transition. The imaging rate is limited by the readout time of our camera. The photoassociation pulse begins halfway between the second and the third images. We use multiple imaging pulses to improve statistics and to partially correct for small losses other than those due to the photoassociation pulse. These losses are typically 4% between images, most likely due to three-body losses and the imaging light. Once the number of atoms is extracted from the images [14], we calculate f, the fraction of atoms remaining after the photoassociation pulse.

Figure 2 shows a typical photoassociation spectrum. Each point represents a freshly prepared condensate. We use a Fabry-Perot etalon and a reference laser locked to an atomic Na line to measure differences in the photoassociation frequency with a precision of 5 MHz. The laser linewidth is <3 MHz. All detunings quoted are relative to the center of the photoassociation line in the low intensity limit. For small trap loss, we expect the line to be Lorentzian (in contrast to photoassociation lines in an uncondensed thermal sample where the kinetic energy distribution distorts the line shape [15]). For significant trap loss, as in Fig. 2, one must account for the change of the density profile during the photoassociation pulse.

The two-body photoassociation process changes the local atomic density as $\dot{n}(t, \mathbf{r}) = -K(I, \omega) n^2(t, \mathbf{r})$, where $K(I, \omega)$ is the intensity and frequency dependent photoassociation rate constant. Because the characteristic time for the motion of the atoms, the trap oscillation period, is long compared to the photoassociation pulse, we can assume that the local density changes only due to photoassociation, and

$$n(t, \mathbf{r}) = \frac{n(0, \mathbf{r})}{1 + K(I, \omega) n(0, \mathbf{r}) t} . \tag{1}$$

The density distribution flattens with time. Spatially integrating Eq. (1), assuming an initial, parabolic (Thomas-Fermi), density distribution and a uniform intensity I, leads to an expression for the fraction of atoms remaining in the condensate:

$$f(\eta) = \frac{15}{2} \eta^{-5/2} \left\{ \eta^{1/2} + \frac{1}{3} \eta^{3/2} - (1 + \eta)^{1/2} \tanh^{-1} \left[\sqrt{\eta/(1 + \eta)} \right] \right\}, \tag{2}$$

where $\eta = K(I, \omega) n(0, \mathbf{0}) t = K_m(I) n(0, \mathbf{0}) t / (1 + \{2[\omega - \omega_0(I)]/\gamma(I)\}^2)$. We use a three parameter fit of Eq. (2) to the spectra to extract the on-resonance rate constant $K_m(I)$, effective linewidth $\gamma(I)$, and central frequency $\omega_0(I)$ (for example, the dotted line in Fig. 2). The fit is good. To further verify Eq. (2), we plot the measured $1 - f$ as a function of pulse length for $I = 140$ W cm^{-2} and $\omega = \omega_0$, along with a one parameter (K_m) fit to the data (Fig. 3). The fitting uncertainties are indicated.

By fitting spectra obtained at various intensities, we measure $K_m(I)$, $\gamma(I)$, and $\omega_0(I)$. Following [16] we calculate the unbroadened molecular linewidth of the chosen state to be $\gamma_0/2\pi = 18.5$ MHz (nearly twice the atomic linewidth). This is in good agreement with the measured linewidth of 19.5(25) MHz in the low intensity limit, where it is independent of intensity. At higher intensities, we observe broadening with a maximum linewidth of 60 MHz at 1 kW cm^{-2}. Homogeneous power broadening is calculated to be 3 orders of magnitude too low to explain this width. It is, however, partially explained by differential light shifts of the unresolved molecular hyperfine states. These states are calculated to be split by less than 1 MHz at low intensities and about 30 MHz at our maximum intensity. Another possible contribution is the inhomogeneity of the photoassociation beam intensity combined with the large light shift (discussed below). Variations due to either local spatial inhomogeneity (e.g.,

interference fringes) or displacement of the cloud from the center of the Gaussian beam could account for the extra width. Assuming these inhomogeneous broadening mechanisms do not change the area of the line (verified by a simulation), we take the on-resonance photoassociation rate constant to be $K_0(I) = K_m(I)\gamma(I)/\gamma(I \to 0)$.

Figure 4 shows corrected and uncorrected rate constants as a function of intensity (for various pulse lengths). The error bars are the fitting uncertainties. Once we correct for the inhomogeneous broadening we get a linear dependence on intensity with a slope of $dK_0/dI = 3.5(2)(10) \times 10^{-10}$ $(\mathrm{cm^3\,s^{-1}})/(\mathrm{kW\,cm^{-2}})$. The uncertainties are due, respectively, to fitting and to the combined uncertainties in the measurement of the intensity and density. For intensities above 1.2 $\mathrm{kW\,cm^{-2}}$, which we could achieve only by more tightly focusing the photoassociation laser, atomic dipole forces significantly perturb the condensate, thwarting meaningful measurements. A coupled-channels, two-body scattering calculation with no adjustable parameters [17] yields a photoassociation rate constant of $dK_0/dI = 4.1 \times 10^{-10}$ $(\mathrm{cm^3\,s^{-1}})/(\mathrm{kW\,cm^{-2}})$ for our range of intensities. This includes a factor of 2 decrease relative to a noncondensed gas and agrees well with our experimental result.

We study the photoassociation light shift, previously observed in a noncondensed gas [18], in a set of experiments where the total fluence (intensity $\times$ pulse length) of the pulse was kept constant, to maintain the depth of the photoassociation dip in an easily observable regime. The results are shown in Fig. 5. The measured light shift is $-164(35)$ $\mathrm{MHz}/(\mathrm{kW/cm^2})$, which leads at high intensity to a shift large compared to the linewidth. The principal contribution to the uncertainty is the intensity calibration. During preparation of this work, we became aware of similar results in lithium [19].

While the strength of the photoassociation resonance is dominated by s-wave scattering, the dominant contribution to the light shift is due to a d-wave shape resonance. A theoretical calculation of the light shifts using Eq. (3.7) of Ref. [20], including the effect of the d-wave shape resonance embedded in the continuum, gives an average value of -130 $\mathrm{MHz}/(\mathrm{kW/cm^2})$ with a spread of ± 13 $\mathrm{MHz}/(\mathrm{kW/cm^2})$ due to the hyperfine structure.

We now consider the upper limit to the photoassociation rate constant K_0 [this implies a lower limit on the photoassociation time $\tau = (K_0 n)^{-1}$]. If one uses a semiclassical theory that is commonly applied to collisions of laser-cooled atoms [21], then $K = \sigma v = \pi R_C^2 P v$, where R_C is the Condon radius (see Fig. 1), and P is the probability of a photoassociative transition with a maximum value of 1. If we take the relative velocity v of the atoms to be $h/(2mr_y) = 0.6$ $\mathrm{mm\,s^{-1}}$, where m is the atomic mass, then the maximum photoassociation rate constant is 4 orders of magnitude lower than our highest measured value. This reveals the inadequacy of a semiclassical approach, which fails to take into account threshold laws [10].

Quantum theories for the photoassociation rate constant can be compared by expressing K as $K = (h/m)L$, where L is a characteristic length. Two-body s-wave scattering theory for a BEC gives $L_s = |S(k)|^2/k$, where $\hbar k$ is the relative collision momentum and $S(k)$ is the S-matrix element for atom loss via photoassociation. References [20,22] show that, on resonance,

$$L_s(I) = \frac{4\gamma_0 \Gamma(k,I)/k}{[\gamma_0 + \Gamma(k,I)]^2}, \tag{3}$$

where $\hbar\Gamma(k,I) = 2\pi|\langle e|\hbar\Omega|k\rangle|^2$ is the Fermi-golden-rule stimulated-decay width of the excited molecular state $|e\rangle$ due to the optical coupling $\hbar\Omega \propto \sqrt{I}$ with the colliding atoms. Since $\Gamma \propto k$ as $k \to 0$, and $\Gamma/\gamma_0 < 0.001$ in our range of power and collision energy, L_s is independent of k. L_s is linear in I for our experimental conditions, and dL_s/dI is calculated to be $24\,\mathrm{nm}/(\mathrm{kW/cm^2})$. This gives the above-quoted rate constant in good agreement with the experiment. In our power range, L_s can be significantly

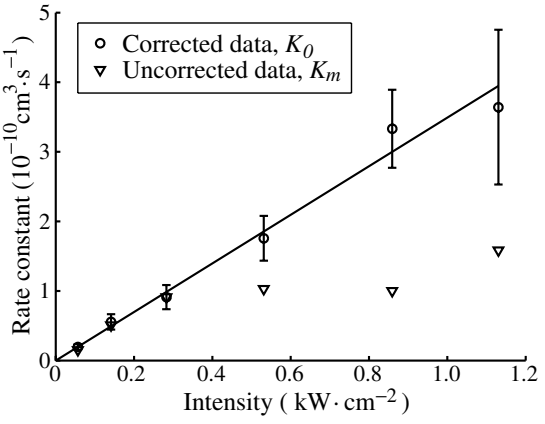

FIG. 4. Resonant photoassociation rate constant as a function of intensity. The corrected data has been adjusted to account for the inhomogeneous broadening.

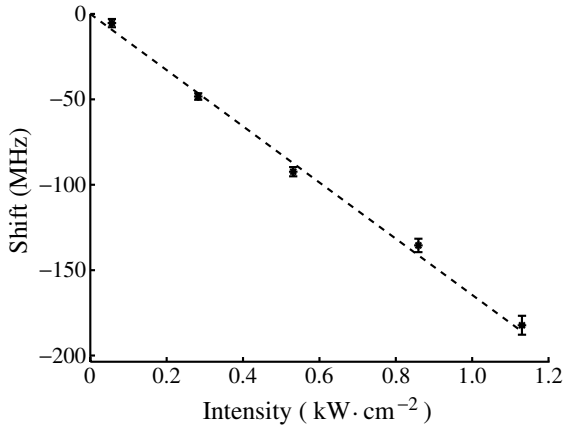

FIG. 5. The light shift of the resonance as a function of laser intensity.

larger than the Condon point for the transition, 2.0 nm. Note that Eq. (3) shows that $L_s(I)$ will saturate with increasing I and decrease for sufficiently large I.

The upper limit to the two-body quantum K_0 is the unitarity limit where $|S|^2 = 1$ so $L_u = 1/k = \lambda/2\pi$, where λ is the de Broglie wavelength. Since λ is on the order of the BEC size $L_s/L_u \ll 1$, thus our experiment is well below the unitarity constraint.

Recent many-body theoretical work [3,23,24] has suggested an upper limit to K_0 in a BEC of $K_0 \sim \frac{h}{m} L_J$, where $L_J = \frac{n^{-1/3}}{2\pi}$ and $n^{-1/3}$ is the mean distance between particles. One might question if two-body scattering methods are applicable at densities where L_s becomes larger than L_J. At our maximum density $L_J = 22$ nm, so $L_s/L_J \approx 1$ at our highest intensities. Nevertheless, the linearity of $K_0(I)$ (Fig. 4) shows that, with our experimental uncertainty, we have no evidence for the failure of two-body theory.

Larger values of L_s/L_J might be accessible by a modification to our experimental design. We can use the atomic dipole force (which currently limits our ability to use high intensities) to our advantage by trapping the atoms with the photoassociation laser. Without changing the atomic dipole forces, the laser can be suddenly brought from far off molecular resonance to on molecular resonance to induce photoassociation. Difficulties due to the molecular light shift might be reduced by finding a transition with a smaller light shift.

In conclusion, we have measured the single-photon photoassociation in a BEC, in good agreement with two-body theory. This agreement represents a confirmation of the factor-of-two reduction for a two-body inelastic process in a BEC. The characteristic time for photoassociation is as short as 5 μs, much shorter than the 100 μs to traverse the mean distance between atoms, another demonstration of the extreme quantum nature of the collisions. Our largest rate is still much smaller than the unitarity limit, but is on the order of a limit suggested on the basis of many-body effects; however, we have yet to see the effects of this limit.

We acknowledge funding support from the U.S. Office of Naval Research and NASA. J. H. D. and H. H. acknowledge funding from the Alexander von Humboldt foundation. A. B. was partially supported by DGA (France).

*Institut für Experimentalphysik, Universität Innsbruck, Technikerstrasse 25, A-6020 Innsbruck, Austria.
†The Institute of Optics, University of Rochester, Rochester, NY 14627.
‡Naval Research Laboratory, Washington, D.C. 20375.
§Department of Physics, Williams College, Williamstown, MA 01267.
‖Bell Laboratories, Lucent Technologies, Holmdel, NJ 07733.
¶Department of Physics, Korea University, 5-1 Ka Anam-dong, Sungbuk-ku, Seoul 136-701, Korea.
**INFM and LENS, Università di Firenze, Largo E. Fermi 2, I-50125, Firenze, Italy.

[1] M. H. Anderson, J. R. Ensher, M. R. Matthews, C. E. Wieman, and E. A. Cornell, Science **269**, 198 (1995).
[2] K. B. Davis, M.-O. Mewes, M. R. Andrews, N. J. van Druten, D. S. Durfee, D. M. Kurn, and W. Ketterle, Phys. Rev. Lett. **75**, 3969 (1995).
[3] M. Koštrun, M. Mackie, R. Côté, and J. Javanainen, Phys. Rev. A **62**, 063616 (2000).
[4] D. J. Heinzen, R. Wynar, P. D. Drummond, and K. V. Kheruntsyan, Phys. Rev. Lett. **84**, 5029 (2000).
[5] E. Timmermans, P. Tommasini, R. Côté, M. Hussein, and A. Kerman, Phys. Rev. Lett. **83**, 2691 (1999).
[6] P. S. Julienne, K. Burnett, Y. B. Band, and W. C. Stwalley, Phys. Rev. A **58**, R797 (1998).
[7] K. Helmerson and L. You, Phys. Rev. Lett. **87**, 170402 (2001).
[8] R. Wynar, R. S. Freeland, D. J. Han, C. Ryu, and D. J. Heinzen, Science **287**, 1016 (2000).
[9] J. M. Gerton, D. Strekalov, I. Prodan, and R. G. Hulet, Nature (London) **408**, 692 (2000).
[10] J. Weiner, V. S. Bagnato, S. Zilio, and P. S. Julienne, Rev. Mod. Phys. **71**, 1 (1999).
[11] Unless otherwise stated, all uncertainties reported here are one standard deviation combined systematic and statistical uncertainties.
[12] M. Kozuma, L. Deng, E. W. Hagley, J. Wen, R. Lutwak, K. Helmerson, S. L. Rolston, and W. D. Phillips, Phys. Rev. Lett. **82**, 871 (1999).
[13] M. R. Andrews, M.-O. Mewes, N. J. van Druten, D. S. Durfee, D. M. Kurn, and W. Ketterle, Science **273**, 84 (1996).
[14] Because we are in a regime where the phase shift of the light passing through the BEC is large (up to several radians), the extracted density is a multivalued function of the phase contrast signal. We assume a Thomas-Fermi distribution for the atoms to resolve this ambiguity.
[15] K. M. Jones, P. D. Lett, E. Tiesinga, and P. S. Julienne, Phys. Rev. A **61**, 012501 (2000).
[16] M. Movre and G. Pichler, J. Phys. B **13**, 697 (1980).
[17] C. Samuelis, E. Tiesinga, T. Laue, M. Elbs, H. Knöckel, and E. Tiemann, Phys. Rev. A **63**, 012710 (2001).
[18] K. M. Jones, S. Maleki, L. P. Ratliff, and P. D. Lett, J. Phys. B **30**, 289 (1997).
[19] J. M. Gerton, B. J. Frew, and R. G. Hulet, Phys. Rev. A **64**, 053410 (2001).
[20] J. L. Bohn and P. S. Julienne, Phys. Rev. A **60**, 414 (1999).
[21] A. Gallagher and D. E. Pritchard, Phys. Rev. Lett. **63**, 957 (1989).
[22] J. L. Bohn and P. S. Julienne, Phys. Rev. A **54**, R4637 (1996).
[23] J. Javanainen and M. Mackie, cond-mat/0108349, 2001.
[24] J. Javanainen (private communication).